Viscous Stabilization of Gravity Wave Critical Level Flows

DAVID C. FRITTS AND MARVIN A. GELLER[1]

Laboratory for Atmospheric Research, University of Illinois, Urbana 61801

(Manuscript received 21 May 1976, in revised form 10 August 1976)

ABSTRACT

A criterion for the viscous stabilization of gravity wave critical level flow is derived to be $Z_{\frac{1}{2}} \leqslant 2.5\, Z_\nu$, where $Z_{\frac{1}{2}}$ is the vertical thickness of the unstable region in the vicinity of a gravity wave critical level calculated with an inviscid linear theory and Z_ν is the viscous length scale for gravity wave critical level interaction. The stability implications of this criterion are examined for gravity wave critical level flows in the laboratory, the atmospheric planetary boundary layer, the upper atmosphere and the ocean thermocline region. Laboratory flows, where no tubulence in the vicinity of a gravity wave critical level was observed, are found to meet our criterion for stability. Applying this criterion to atmospheric boundary layer flows implies that no such regions of instability should be observed in the fully developed turbulent convective region, but such turbulent regions should exist in stably stratified cases. Using observed gravity wave parameters for the upper atmosphere the stability criterion gives the result that molecular viscosity should stabilize gravity wave critical level flows above about 130 km altitude. Using gravity wave parameters appropriate to the ocean in the theory suggests that gravity wave critical level instabilities might give rise to some of the thin mixed layers that are observed in the thermocline region.

1. Introduction

A well-known property of linear steady-state analysis of gravity wave critical level flow (e.g., Booker and Bretherton, 1967; Hines, 1968) is that the internal gravity wave flow is unstable in the vicinity of critical levels. This instability is a result of the large vertical shears in the wave's horizontal velocity as well as large vertical derivatives of temperature that develop close to the critical level where the wave's horizontal trace velocity becomes equal to the mean flow velocity. Geller, Tanaka and Fritts (1975, hereafter referred to as GTF), explored this mechanism through the use of two computational models. One of these was an analytic linear inviscid model and the other was a numerical nonlinear, almost inviscid (high Reynolds number) model. It is the purpose of the present paper to examine the effects of dissipation on this instability mechanism that was investigated by GTF.

The dissipation investigated is that resulting from molecular viscosity and heat conduction. The inclusion of this dissipation eliminates the singular nature of the gravity wave critical level problem and hence, does away with the infinite shears that appear in the linear, nondissipative, critical level formulation. We wish to find out under what conditions the inclusion of dissipation in the critical level problem smooths out the gravity wave behavior close to the critical level sufficiently to eliminate the instability studied by GTF.

[1] Also affiliated with the Aeronomy Laboratory, University of Illinois.

2. Viscous Model

Hazel (1967) was the first to solve the gravity wave critical level problem including the effects of viscosity and heat conduction. His method of solution involved matching asymptotic solutions away from the critical level to a numerically integrated solution of the appropriate sixth-order differential equation. We use a different approach in which solutions of the sixth-order differential equation near the critical level are expressed as power series. This solution is then matched to the asymptotic forms found to be valid far from the critical level. This method of solution is now described.

We start with essentially the same equations as in Hazel (1967):

$$u_t+Uu_x+wU_z+\frac{1}{\bar{\rho}}p_x-\nu\nabla^2u=0 \qquad (1)$$

$$w_t+Uw_x+\sigma+\frac{1}{\bar{\rho}}p_z-\nu\nabla^2w=0 \qquad (2)$$

$$u_x+w_z=0 \qquad (3)$$

$$\sigma_t+U\sigma_x-N^2w-K\nabla^2\sigma=0. \qquad (4)$$

In writing Eqs. (1)–(4), the mean flow velocity is given by $[U(z),0]$, the perturbation velocity is $[u(x,z,t),w(x,z,t)]$; $\bar{\rho}(z)$ is the basic-state density and ρ the perturbation density; p is perturbation pressure; $\sigma=g\rho/\bar{\rho}$ is the buoyancy acceleration; N is the Brunt-Väisälä frequency; and ν and K are the coefficients of kinematic viscosity and thermal conduction, respectively. The t, x and z subscripts indicate partial derivatives with respect to these variables. Assuming all perturbation quantities to vary as $e^{i\alpha(x-ct)}$ and eliminating u, σ, and p in Eqs. (1)–(4) gives Hazel's corrected equation (1.5):

$$\left[i\alpha(U-c)-K\left(\frac{d^2}{dz^2}-\alpha^2\right)\right]\left\{\left[-i\alpha(U-c)+\nu\left(\frac{d^2}{dz^2}-2\alpha^2\right)\right]\frac{d^2}{dz^2}+i\alpha[U_{zz}+\alpha^2(U-c)]+\nu\alpha^4\right\}w+\alpha^2N^2w=0. \quad (5)$$

Viscous effects become increasingly important as the critical level is approached since in the linear inviscid theory the gravity wave's vertical wavelength goes linearly to zero at the critical level. For this reason we make the same simplifying assumption as Hazel (1967), that $\alpha \ll d/dz$. For simplicity we also consider a linear wind shear so that $U-c=U_z z$, where $z=0$ at the critical level. Also following Hazel, a viscous length scale is defined as the level where the inertial terms balance the viscous term in Eq. (1). This gives

$$Z_\nu \equiv \left(\frac{\nu}{\alpha U_z}\right)^{\frac{1}{3}}. \quad (6)$$

With the above simplifications and with $z=Z_\nu\zeta$, Eq. (5) becomes Hazel's Eq. (1.7):

$$\left[\left(iP^{-1}\frac{d^2}{d\zeta^2}+\zeta\right)\left(i\frac{d^2}{d\zeta^2}+\zeta\right)\frac{d^2}{d\zeta^2}+\overline{\mathrm{Ri}}\right]w=0. \quad (7)$$

Here $P=\nu/K$ is the Prandtl number and $\overline{\mathrm{Ri}}=N^2/U_z^2$ the Richardson number of the basic state.

As in GTF, we wish to solve Eq. (7) and use the local instantaneous Richardson number as defined by

$$\mathrm{Ri}=-\frac{\dfrac{g}{(\bar{\rho}+\rho)}\dfrac{\partial}{\partial z}(\bar{\rho}+\rho)}{\left(U_z+\dfrac{\partial u}{\partial z}\right)^2} \quad (8)$$

as a measure of the stability of the basic state plus the gravity wave perturbation.

Our method of solving Eq. (7) is to match outer asymptotic solutions ($|\zeta|\gg 1$) to the power series solutions. This is preferable to the approach used by Hazel (1967) for our purposes since we will want to form derivatives of our solution to obtain Ri.

The form of Eq. (7) suggests that asymptotic solutions exist of form $\zeta^m \exp(q\zeta^{\frac{3}{2}})$ (Hazel, 1967; Koppel, 1964). A bit of mathematical manipulation gives these asymptotic solutions as

$$\left.\begin{aligned}
w_1&=A_1\zeta^{\frac{1}{2}+i\mu}[1+O(\zeta^{-3})]\\
w_2&=A_2\zeta^{\frac{1}{2}-i\mu}[1+O(\zeta^{-3})]\\
w_3&=A_3\zeta^{-5/4}\exp(-\tfrac{2}{3}i^{\frac{1}{2}}\zeta^{\frac{3}{2}})[1+O(\zeta^{-3})]\\
w_4&=A_4\zeta^{-5/4}\exp(\tfrac{2}{3}i^{\frac{1}{2}}\zeta^{\frac{3}{2}})[1+O(\zeta^{-3})]\\
w_5&=A_5\zeta^{-9/4}\exp[\tfrac{2}{3}(iP)^{\frac{1}{2}}\zeta^{\frac{3}{2}}][1+O(\zeta^{-3})]\\
w_6&=A_6\zeta^{-9/4}\exp[-\tfrac{2}{3}(iP)^{\frac{1}{2}}\zeta^{\frac{3}{2}}][1+O(\zeta^{-3})]
\end{aligned}\right\}, \quad (9)$$

where $\mu=(\overline{\mathrm{Ri}}-\frac{1}{4})^{\frac{1}{2}}$. w_1 and w_2 correspond to the inviscid critical level solutions of Booker and Bretherton (1967), while w_3, w_4, w_5 and w_6 represent "viscous" and "heat conduction" solutions. Note that w_4 and w_6 decay as $\zeta\rightarrow+\infty$ and w_3 and w_5 decay as $\zeta\rightarrow-\infty$. This set of equations [(9)] defines the outer solution.

The inner solution is obtained by noting that Eq. (7) is nonsingular at $\zeta=0$ and thus the power series

$$w=\sum_{n,\gamma} a_{n,\gamma}\zeta^{n+\gamma}$$

should be a valid solution for bounded ζ. Substituting this into Eq. (7) implies the following relation:

$$\begin{aligned}
\sum_{n,\gamma}\{&-P^{-1}a_{n+6,\gamma}(n+\gamma+6)(n+\gamma+5)(n+\gamma+4)\\
&\times(n+\gamma+3)(n+\gamma+2)(n+\gamma+1)+i(1+P^{-1})a_{n+3,\gamma}\\
&\times(n+\gamma+3)(n+\gamma+2)(n+\gamma+1)(n+\gamma)\\
&+2iP^{-1}a_{n+3,\gamma}(n+\gamma+3)(n+\gamma+2)(n+\gamma+1)\\
&+a_{n,\gamma}[(n+\gamma)(n+\gamma-1)+\overline{\mathrm{Ri}}]\}\zeta^{n+\gamma}=0. \quad (11)
\end{aligned}$$

Equating the coefficients of like powers of ζ to zero gives a set of recursion relations for the $a_{n,\gamma}$. Taking all $a_{n,\gamma}=0$ for $n<0$, we find to lowest order that

$$-P^{-1}a_{0,\gamma}\gamma(\gamma-1)(\gamma-2)(\gamma-3)(\gamma-4)(\gamma-5)=0. \quad (12)$$

Thus, if $a_{0,\gamma}\neq 0$, γ may assume the values 0, 1, 2, 3, 4 and 5, leading to six independent power series solutions to Eq. (7), each of the form

$$w_\gamma=B_\gamma\sum_n a_{n,\gamma}\zeta^{n+\gamma}, \quad (13)$$

where $a_{n,\gamma}=0$ for $n<0$, $a_{0,\gamma}=1$, and

$$a_{n,\gamma}=\frac{i[P(n+\gamma-6)+(n+\gamma-4)]a_{n-3,\gamma}}{(n+\gamma)(n+\gamma-1)(n+\gamma-2)}+\frac{P[(n+\gamma-6)(n+\gamma-7)+\overline{\mathrm{Ri}}]a_{n-6,\gamma}}{(n+\gamma)(n+\gamma-1)(n+\gamma-2)(n+\gamma-3)(n+\gamma-4)(n+\gamma-5)}. \quad (14)$$

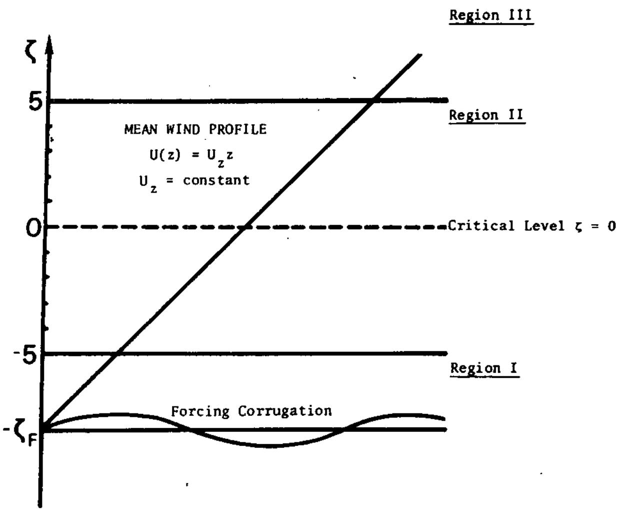

FIG. 1. Geometry of the viscous critical level problem.

The unknown coefficients in (9) and (13) are still to be determined from matching the inner solutions to the outer solutions.

The geometry of the viscous critical level problem treated in this paper is illustrated in Fig. 1. Region I is pictured as that region where $\zeta < -5$. Region II is where $|\zeta| \leqslant 5$ and region III is where $\zeta > 5$. The reason for this choice stems from the asymptotic solutions in expression (9) being valid to order ζ^{-3}. Thus, we expect the outer solutions to be valid to about 1% accuracy for $|\zeta| \geqslant 5$. Given our inner and outer solutions for w, we now need to apply the lower boundary condition that results from our method of forcing, the upper boundary condition at $\zeta \rightarrow \infty$, and the matching conditions at $\zeta = -5$ and $\zeta = +5$.

In region I, we take our solution to be of the form

$$w_{\mathrm{I}}(\zeta) = A_1\zeta^{\frac{1}{2}+i\mu} + A_2\zeta^{\frac{1}{2}-i\mu} + A_3\zeta^{-5/4}\exp(\tfrac{2}{3}i^{\frac{1}{2}}\zeta^{\frac{3}{2}}) + A_5\zeta^{-9/4}\exp[\tfrac{2}{3}(iP)^{\frac{1}{2}}\zeta^{\frac{3}{2}}]. \quad (15)$$

Thus, we allow for an incident wave propagating energy from below, a reflected wave and both downward decaying solutions. Since we wish to apply a radiation condition at $\zeta \rightarrow +\infty$, the outer solution in region III is taken to be

$$w_{\mathrm{III}}(\zeta) = C_1\zeta^{\frac{1}{2}+i\mu} + C_4\zeta^{-5/4}\exp(-\tfrac{2}{3}i^{\frac{1}{2}}\zeta^{\frac{3}{2}}) + C_6\zeta^{-9/4}\exp[-\tfrac{2}{3}(iP)^{\frac{1}{2}}\zeta^{\frac{3}{2}}]. \quad (16)$$

All six inner solutions are retained in region II:

$$w_{\mathrm{II}} = \sum_{\gamma=0}^{5} B_\gamma \sum_{n=0}^{\infty} a_{n,\gamma}\zeta^{n+\gamma}. \quad (17)$$

In this paper, we retain the terms in the power series for $n \leqslant 27$ as we wish the accuracy of both the inner and outer solutions to be on the order of 1%. Thus, we require 13 relations to determine 13 constants, the A's, B's and C's.

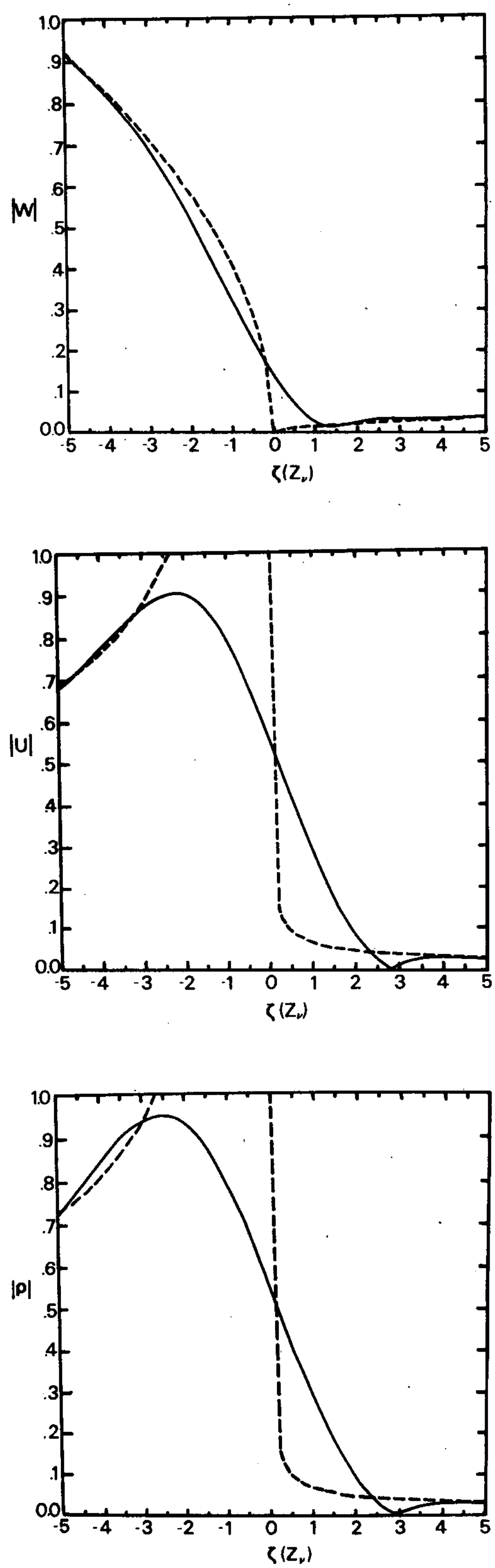

FIG. 2. Behavior of the amplitude of the gravity wave variables w (top), u (middle) and ρ (bottom) in the vicinity of the critical level $\zeta = 0$ for the inviscid (dashed line) and viscous (solid line) calculations. Units for the variables are arbitrary.

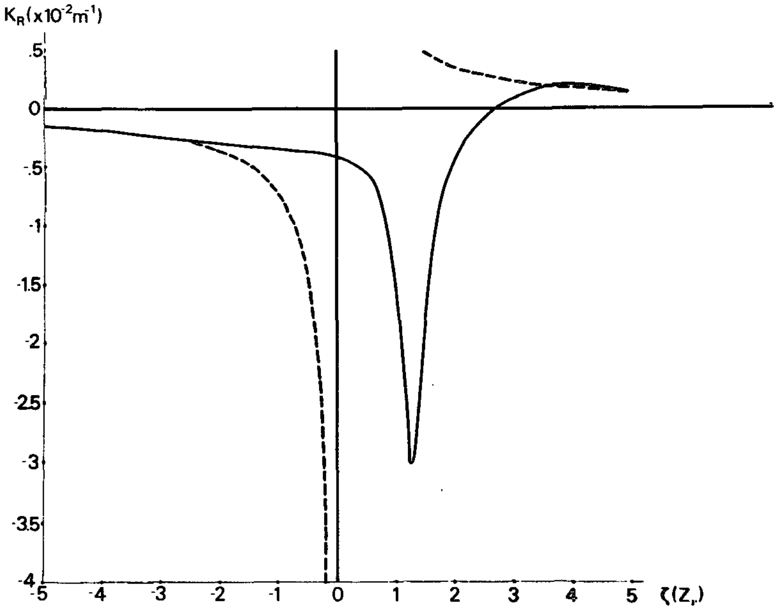

FIG. 3. Behavior of the gravity wave wavenumber k_r in the vicinity of the critical level for the inviscid (dashed line) and viscous (solid line) calculations.

Twelve of the 13 necessary equations are obtained by requiring continuity of w and its first five derivatives across the interface between regions I and II, as well as that between II and III. The 13th equation is the lower boundary condition which specifies the vertical velocity induced by motion over a sinusoidally corrugated rigid boundary as in GTF. This lower boundary condition is applied at the level $Z_f = Z_r \zeta_f$.

Solving for the 13 constants yields an expression for w in all regions. All other perturbation quantities can be found from this. The local instantaneous Richardson number is then obtained by the use of Eq. (8).

3. Results

Before comparing the geometry of the unstable regions calculated by GTF with those of the present paper, we will first compare the structure of the gravity wave in the vicinity of the critical level computed with and without viscous and thermal conduction effects included.

The inviscid model of GTF is essentially the same as that examined by Booker and Bretherton (1967). In such a linear inviscid model of a gravity wave critical level, w, the wave vertical velocity, goes to zero as $\zeta^{\frac{1}{2}}$; u, the wave horizontal velocity, goes to infinity as $\zeta^{-\frac{1}{2}}$; and ρ, the wave fluctuation in density, goes to infinity as $\zeta^{-\frac{1}{2}}$. (Note that in GTF θ is essentially interchangeable with ρ in this paper.) This behavior is illustrated by the dashed curves in Fig. 2. Also, the effective vertical wavenumber goes to infinity as μ/ζ as the critical level is approached in the linear inviscid theory. This is shown by the dashed line in Fig. 3. In the viscous theory this singular behavior is replaced by a continuous variation of the parameters as the critical level is traversed. This is shown by the solid lines in Figs. 2 and 3.

The vertical flux of horizontal momentum $\overline{uw}$ becomes discontinuous by a factor of $-e^{2\pi\mu}$ in the inviscid theory, while as Hazel (1967) has shown in the viscous theory the momentum flux is joined smoothly over an internal viscous layer to the same values as in the inviscid theory outside the layer. This is shown in Fig. 4. Thus, the results of our model of the viscous gravity wave critical level are consistent with those of Hazel (1967). Since we are interested in looking at the stability of the flow near critical levels as in GTF, but with a

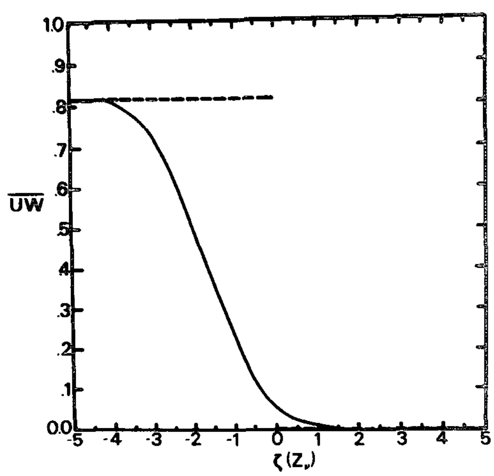

FIG. 4. Behavior of the gravity wave Reynolds' stress $\overline{uw}$ in the vicinity of the critical level for the inviscid (dashed line) and viscous (solid line) calculations.

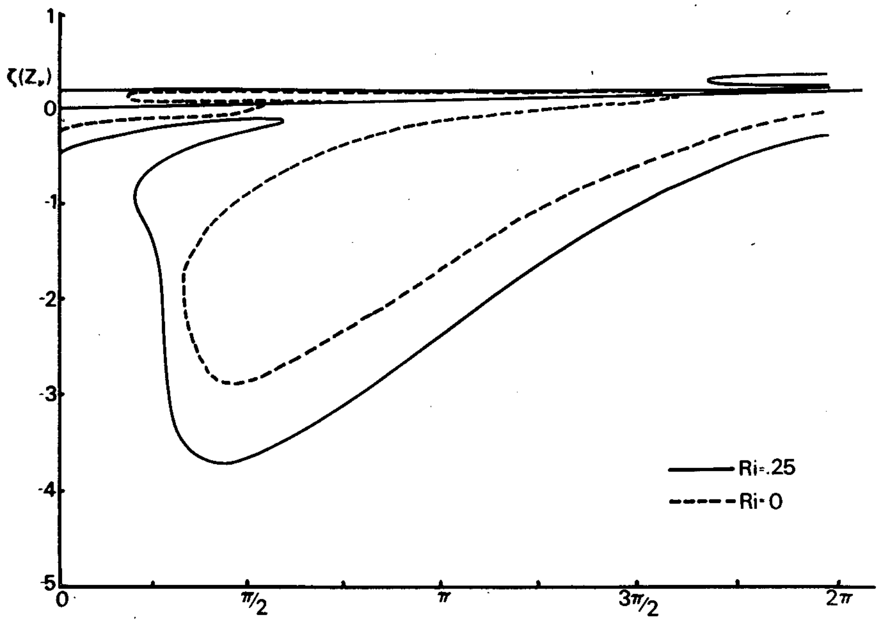

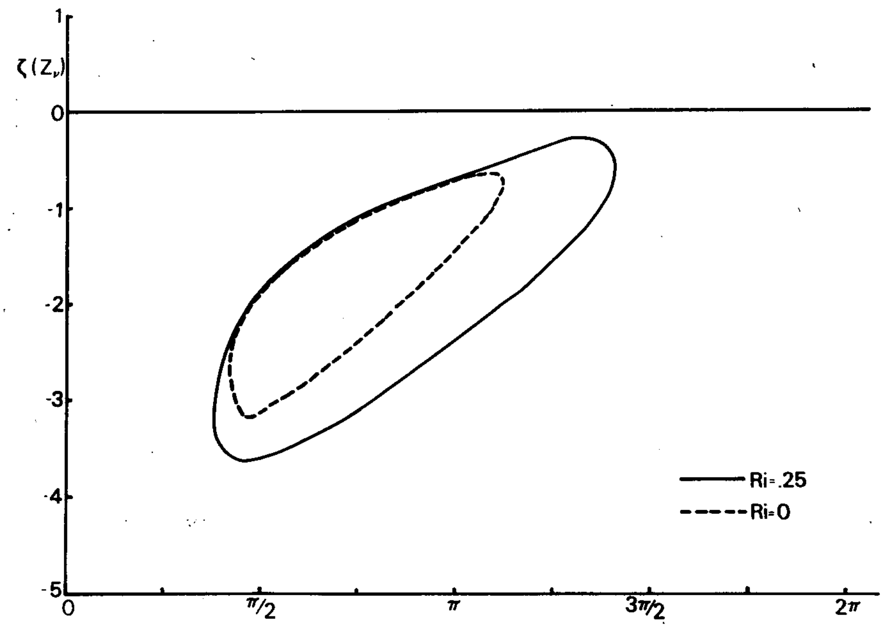

FIG. 5. Configuration of $Ri<\frac{1}{4}$ and $Ri<0$ envelopes about the critical level as given by the inviscid computations (top) and viscous computations (bottom).

viscous theory, a significant difference in our approach is that we have an analytic solution in the critical level region and thus can accurately evaluate derivatives of the wave parameters here.

As in GTF, we wish to examine the region about the critical level where the local instantaneous Richardson number Ri becomes less than 0.25 and 0.00, since these critical values for the Richardson number denote regions where shear instabilities ($Ri<0.25$) and convective instabilities ($Ri<0$) may be expected to develop. These regions are shown in Figs. 5a and 5b for the inviscid and viscous models, respectively. Note that the regions of instability are of somewhat smaller spatial extent with viscous effects included, as would be intuitively expected. The difference in shape of these regions in the immediate vicinity of the critical level is due to the obliteration of the very high shears there by the action of viscosity and heat conduction.

The principal objective of this paper is to obtain a criterion for the viscous stabilization of flow in the immediate vicinity of a gravity wave critical level. We will then check this criterion against the laboratory experiments of Bretherton *et al.* (1967) and Thorpe (1973) for consistency and look at the geophysical implications of this criterion.

In GTF it was anticipated that the relative sizes of Z_ν, the viscous length scale, and $Z_{\frac{1}{4}}$, the maximum depth of the shear instability region, determined whether or not there would exist a region of instability. In Fig. 6 the stabilizing effect of viscosity and heat conduction on the flow near a critical level is illustrated by plotting the envelopes of regions where $\mathrm{Ri}<\frac{1}{4}$ for flow near a critical level for fixed viscosity and thermal conductivity but variable forcing amplitudes. The parameters used for these calculations were as follows: $\nu=6.5\ \mathrm{m^2\,s^{-1}}$, $P=1$, $\alpha=0.4\times10^{-3}\ \mathrm{m^{-1}}$, $U_z=0.024028\ \mathrm{s^{-1}}$ and $N^2=0.000722\ \mathrm{s^{-2}}$. This choice of parameters leads to a viscous length scale Z_ν of 87.8 m and a basic state Richardson number $\overline{\mathrm{Ri}}$ of 1.25. The envelopes where $\mathrm{Ri}<\frac{1}{4}$ were calculated according to the procedure discussed in Section 2 of this paper, where the forcing is imposed 5 km below the critical level and the amplitude W_0, of the vertical motion, assumes in turn the values 4, 2, 1.5 and 1.4 m s^{-1}. The $\mathrm{Ri}<\frac{1}{4}$ envelopes are seen to decrease much faster than the $W_0^{\frac{2}{3}}$ law derived in the Appendix of GTF for inviscid flow. For $W_0\leqslant1.3$ m s^{-1} no region where $\mathrm{Ri}<\frac{1}{4}$ exists, so the action of viscosity and heat conduction has stabilized the flow.

In analyzing the results shown in Fig. 6 we wish to compare $Z_{\frac{1}{4}}$ with Z_ν. There are two methods which may be utilized for this. One way to obtain $Z_{\frac{1}{4}}$ would be by using the simple analytical inviscid critical level model that was presented in GTF. Another method is to utilize the asymptotic expression for $Z_{\frac{1}{4}}$ that was derived in the Appendix to GTF. This relation may be written as

$$Z_{\frac{1}{4}}\sim\left(\frac{W_0^2\overline{\mathrm{Ri}}}{\alpha^2 Z_f U_z^2}\right)^{\frac{1}{3}} \tag{18}$$

from Eq. (A15) in GTF. It should be pointed out that this asymptotic relation only holds in shear regions where

$$\alpha^2\ll\frac{N^2}{(U-c)^2}. \tag{19}$$

To determine the constant of proportionality, we have utilized the inviscid analytic model in GTF for three values of W_0 with all other parameters fixed. This calculation gives the results shown as circled points in Fig. 7. The straight line passing through these points is obtained by the relation

$$Z_{\frac{1}{4}}=1.32\left(\frac{W_0^2\overline{\mathrm{Ri}}}{\alpha^2 Z_f U_z^2}\right)^{\frac{1}{3}}. \tag{20}$$

Eq. (20) should give reasonably accurate values for $Z_{\frac{1}{4}}$ in regions where the inequality (19) is satisfied. Using Eq. (20) for the parameters of Fig. 6 suggests that the condition for the viscous stabilization of the flow near a gravity wave critical level is

$$Z_{\frac{1}{4}}\lesssim2.5Z_\nu. \tag{21}$$

We have found the criterion of Eq. (21) to be valid for several other simulations of linear viscous critical level flow using many different parameters and believe it to be a general criterion for stabilization of gravity wave critical level flows.

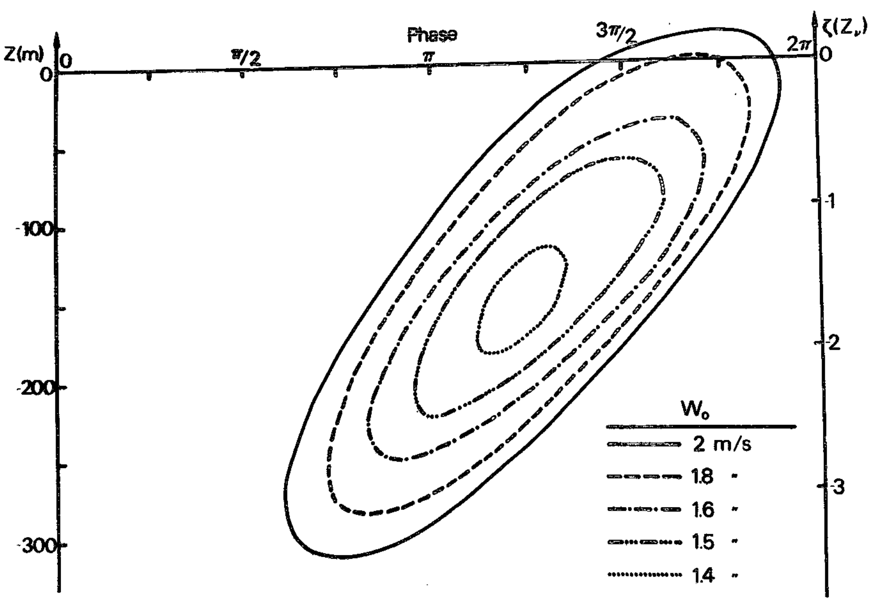

FIG. 6. Configuration of $\mathrm{Ri}<\frac{1}{4}$ envelopes about the critical level calculated with the viscous model with successively decreasing vertical velocity forcing amplitudes W_0. No region where $\mathrm{Ri}<\frac{1}{4}$ exists for $W_0\leqslant1.3$ m s^{-1} in this case.

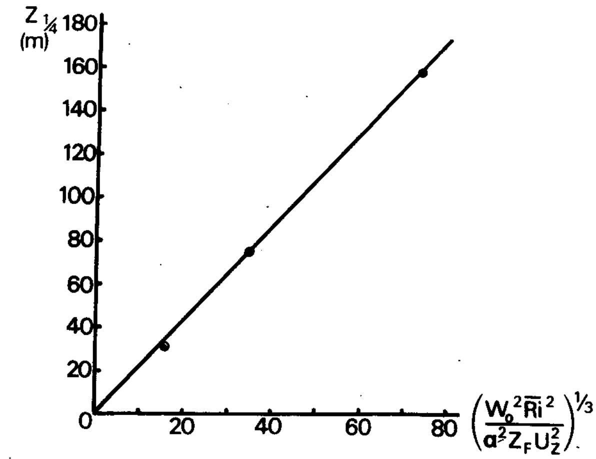

FIG. 7. The best-fit linear relationship of Eq. (20) applied to calculations (points) of $Z_{\frac{1}{4}}$ by the analytic model of GTF.

4. Discussion of stability criterion

Having determined mathematically that $Z_{\frac{1}{4}} \leqslant 2.5 Z_\nu$ should be a criterion for stability of flow in the vicinity of an internal gravity wave critical level, we now wish to see if there is any observational support for this criterion. We are aware of two sets of gravity wave critical level experiments which have been reported by Bretherton *et al.* (1967) and Thorpe (1973). Both experiments were carried out in the same manner. First, a constant vertical density gradient is set up in a long rectangular tube with a small double-sided, wedge-shaped obstacle placed near the center of the bottom of the tube. A linear shear flow is then set up by means of tilting the tube. Gravity waves with zero horizontal trace speed are set up downstream of the obstacle for which a critical level exists at the center of the shear flow. The wave absorption at the critical level is strikingly seen in these experiments. Thorpe (1973) points out, however, that no turbulence was observed at the critical levels. We have performed calculations for four sets of parameters corresponding to the two experiments of Bretherton *et al.* (1967) ($\overline{Ri}=1.2$ and 16.4) and the extreme values of Richardson number in Thorpe's (1973) experiments ($15 \geqslant \overline{Ri} \geqslant 5$). In all cases the value of the computed $Z_{\frac{1}{4}}$ is considerably less than Z_ν, which according to Eq. (21) implies stability of the critical level flow. To carry out these calculations, we used the analytic model of GTF since α was sufficiently large to invalidate the asymptotic expression in Eq. (20). For comparison with parameters that will be quoted later for the atmospheric and oceanic critical level problem, the parameters calculated for the Bretherton *et al.* (1967) experiments with $\overline{Ri}=1.2$ (16.4) were $N^2=12.19$ s^{-2} (0.8918 s^{-2}), $U_z=3.187$ s^{-1} (0.2332 s^{-1}), $W_0=3.044$ cm s^{-1} (0.223 cm s^{-1}), $Z_\nu=0.126$ cm (0.301 cm), which gives $Z_{\frac{1}{4}}=0.018$ cm (0.223 cm). For these calculations, Z_f (or ℓ in the language of GTF) was 5 cm and $\alpha=1.571$ cm^{-1}. For the Thorpe (1973) experiments with $\overline{Ri}=5(15)$, $N^2=2.926$ s^{-2} (0.9753 s^{-2}), $U_z=0.765$ s^{-1} (0.255 s^{-1}) and $W_0=2.338$ cm s^{-1} (0.779 cm s^{-1}). For these calculations Z_f was 8 cm and $\alpha=1.571$ cm^{-1}. This gives $Z_\nu=0.203$ cm (0.292 cm) and $Z_{\frac{1}{4}}<0.08$ cm in both cases (where 0.08 cm was our computer output grid interval). Our criterion of Eq. (21) is found to be consistent with the observed lack of turbulence in the experiments of Bretherton *et al.* (1967) and Thorpe (1973). Of course, it would be very desirable to perform experiments for which Eq. (21) would imply instability of the flow to further check the criterion for viscous stabilization of critical level flow.

GTF's and Tanaka's (1975) calculations of critical level instability were performed for parameters appropriate to the planetary boundary layer. Using these parameters ($\alpha=10^{-3}$ m^{-1}, $\overline{Ri}=2.0819$, $W_0=3$ cm s^{-1} and $U_z=0.024028$ s^{-1}), while assuming that $Z_f=500$ m in Eq. (20), gives $Z_{\frac{1}{4}}=24.6$ m. A quick calculation of the required value of the viscosity that would be required to stabilize the flow according to Eq. (21) implies that the critical level flow is stable if $\nu \geqslant 2.28\times10^{-2}$ m^2 s^{-1}, which is a bit over 1700 times the molecular viscosity at this level in the atmosphere. Usually quoted values for the vertical eddy diffusion coefficient in the planetary boundary layer are several orders of magnitude higher than this critical value of the viscosity, however, (see, e.g., Cuong and Lambert, 1970). These high values for eddy diffusion should be representative of an unstable planetary boundary layer; however, Panofsky (1973) states that, "In stable air, measurable vertical turbulence frequently vanishes above some level between 30 and 150 m; . . ." It is possible then that under stable inversion conditions, after the high levels of daytime turbulence have decayed, for the critical level flow to be unstable. Fukushima *et al.* (1974) have noted in their sodar observations that thin wavy unstable layers are most evident under the strongly stable conditions that exist during nighttime, especially in the period from late fall to winter. We would expect that turbulent regions in the vicinity of critical levels exist in the planetary boundary layer during times when the boundary layer is very stable and convective turbulence has decayed essentially to zero.

GTF suggested from a consideration of the relative sizes of $Z_{\frac{1}{4}}$ and Z_ν that the flow in the vicinity of critical levels should be stabilized by viscous effects in the upper atmosphere at an altitude near 100 km, which is near the turbopause altitude (Blamont and de Jager, 1961). We wish to reexamine this point in light of the criterion for stability of critical level flow derived here. Justus (1973) has derived the magnitudes and horizontal and vertical scales of gravity waves in the upper atmosphere by a method he refers to as the daily difference technique. In particular, he finds the average magnitude of short-period irregular winds U_0 to be in the range

20–45 m s^{-1}, while the horizontal and vertical wavelengths are in the range 100–200 km and 10–20 km, respectively. These values are representative of the altitude region from the bottom of the mesosphere up to about 140 km. Assuming these short irregular wind components to be internal gravity waves, we may estimate W_0 by the relation

$$W_0 \approx \frac{\lambda_z}{\lambda_x} U_0$$

(Hines, 1960), which implies that W_0 is in the range 2–4.5 m s^{-1}. To estimate $Z_{\frac{1}{4}}$ we will use the following parameters in Eq. (21): $\alpha=(2\pi/100)$km, $Z_f=10$ km, $U_z=0.02$ s^{-1} and $\overline{\mathrm{Ri}}=2$; α was chosen from the values from Justus (1973). The choice of Z_f was taken to be approximately one scale height, and U_z and $\overline{\mathrm{Ri}}$ were taken from observations of Rosenberg (1968). Putting these parameters into Eqs. (20) and (21) implies that the criterion for this critical level flow to be stable is

$$\sqrt{\nu} \gtrsim 13.4\, W_0 \text{ [MKS units]}.$$

Thus, the kinematic viscosity must exceed 7.18×10^2 m^2 s^{-1} for $W_0=2$ m s^{-1} and 3.63×10^3 m^2 s^{-1} for $W_0=4.5$ m s^{-1} for stable flow. The molecular viscosity exceeds these values at altitudes of about 120 and 140 km, respectively. It is interesting to note that while turbulence ceases to be visually apparent in rocket vapor trails at about 105 km altitude, Rees *et al.* (1972) have noted evidence for the augmentation of molecular diffusion by turbulent diffusion at altitudes up to 130 km. We conclude then that the flow near gravity wave critical levels should be stabilized by viscosity near the altitude where the effects of turbulence cease to be observed.

It is well established that internal gravity waves commonly exist in the ocean in the vicinity of the thermocline (Phillips, 1966; Fofonoff, 1969). Also, thin layers are also observed in this region (Cooper and Stommel, 1968; Woods and Wiley, 1972). We inquire, in this section as to the relative size of $Z_{\frac{1}{4}}$ and Z_ν in the ocean. To find typical values of internal gravity waves in the ocean, we will use the model of Garrett and Munk (1975). The moored spectra data shown by them imply that waves of 1 h period should have mean vertical displacements on the order of 3 m. This implies that such waves have a vertical velocity amplitude of about 0.1 cm s^{-1}. Consider a wave of 1 h period that might experience a critical level at a depth where the mean current velocity is less than 50 cm s^{-1}. Such a wave will have a wavelength less than 1.8 km. We calculate Z_ν and $Z_{\frac{1}{4}}$ for an internal gravity wave, where $W_0=0.1$ cm s^{-1} and $\alpha=2\pi/(1.8$ km). We also characterize the oceanic state by $U_z=1.6\times10^{-3}$ s^{-1} [estimated from Gulf Stream profiles shown in Stommel (1965, p. 57)], $\overline{\mathrm{Ri}}=10$, $Z_f=500$ m and $\nu=0.01$ cm^2 s^{-1}. Calculations with these parameters give $Z_{\frac{1}{4}}=11.4$ m and $Z_\nu=56.3$ cm. This means that the oceanic flow in the vicinity of critical levels should be unstable to turbulence so long as the thickness of these turbulent layers exceeds 1–2 m (2.5 Z_ν). Thin mixed layers of these dimensions have been observed in the ocean by Cooper and Stommel (1968) and Woods and Wiley (1969).

5. Summary

We have solved a linear critical level model with viscosity and heat conduction to find a criterion for the stabilization of gravity wave critical level flow by viscosity. We find this criterion to be $Z_{\frac{1}{4}} \lesssim 2.5\, Z_\nu$ where $Z_{\frac{1}{4}}$ is the maximum vertical thickness of the unstable (in the $\mathrm{Ri}<\frac{1}{4}$ sense) region and Z_ν is the viscous length scale defined by Hazel (1967).

We have looked at the implications of this criterion for stability of critical level flows in the laboratory, planetary boundary layer, upper atmosphere and ocean thermocline region. Critical level flows that have been observed to be stable in the laboratory are found to satisfy this criterion for stability. This criterion implies that critical level instability should exist in the planetary boundary layer under the stable inversion conditions during which thin turbulent layers have been observed. Calculations for upper atmosphere gravity wave parameters indicate that gravity wave critical level flow should be stable above about 130 km. Using reasonable parameters for internal gravity waves in the ocean it is found that gravity wave instabilities in the ocean should produce thin mixed layers on the order of 1–10 m thick.

Acknowledgments. This paper was written while M. A. Geller was on sabbatical leave at the Division of Atmospheric Science of the Rosenstiel School of Marine and Atmospheric Sciences at the University of Miami in Coral Gables, Fla, and D. C. Fritts was a visitor with the Upper Atmosphere Project of the National Center for Atmospheric Research in Boulder, Colo. We thank both institutions for their hospitality. The computations reported here were done on the CDC 7600 computer at the National Center for Atmospheric Research. This research was supported by the National Science Foundation under Grant DES74-03314A01.

REFERENCES

Blamont, J. E., and C. de Jager, 1961: Upper atmospheric turbulence near the 100 km level. *Ann. Geophys.*, **17**, 134–144.

Booker, J. R., and F. P. Bretherton, 1967: The critical layer for internal gravity waves in a shear flow. *J. Fluid Mech.*, **27**, 513–539.

Bretherton, F. P., P. Hazel, S. A. Thorpe and I. R. Wood, 1967: (Appendix to a paper by P. Hazel). *J. Fluid Mech.*, **30**, 781–784.

Cooper, J. W., and H. Stommel, 1968: Regularly spaced steps in the main thermocline near Bermuda. *J. Geophys. Res.*, **73**, 5849–5854.

Cuong, N. B., and G. Lambert, 1970: Geographical variations of the large-scale vertical exchange speed. *J. Geophys. Res.*, **75**, 2877–2884.

Fofonoff, N. P., 1969: Spectral characteristics of internal waves in the ocean. *Deep-Sea Res.*, **16**, Suppl., 58–71.

Fukushima, M., K. Akita and H. Tanaka, 1974: Sodar probing of small-scale ordered motions appeared in the atmospheric planetary boundary layer. *J. Meteor. Soc., Japan*, **52**, 428–439.

Garrett, C., and W. Munk, 1975: Space-time scales of internal waves: A progress report. *J. Geophys. Res.*, **80**, 291–297.

Geller, M. A., H. Tanaka and D. C. Fritts, 1975: Production of turbulence in the vicinity of critical levels for internal gravity waves. *J. Atmos. Sci.*, **32**, 2125–2135.

Hazel, P., 1967: The effect of viscosity and heat conduction on internal gravity waves at a critical level. *J. Fluid Mech.*, **30**, 775–784.

Hines, C. O., 1960: Internal gravity waves at ionospheric heights. *Can. J. Phys.*, **38**, 1441–1481.

——, 1968: Some consequences of gravity wave critical layers in the upper atmosphere. *J. Atmos. Terr. Phys.*, **30**, 837–843.

Justus, C. G., 1973: Upper atmospheric mixing by gravity waves. AIAA Paper No. 73-495, presented at the Conference on Environmental Impact of Aerospace Operations in the High Atmosphere, June 1973, Denver.

Koppel, D. 1964: On the stability of flow of a thermally stratified fluid under the action of gravity. *J. Math. Phys.*, **5**, 963–982.

Panofsky, H. A., 1973: The boundary layer above 30 m. *Bound.-Layer Meteor.*, **4**, 251–264.

Phillips, O. M., 1966: *The Dynamics of the Upper Ocean.* Cambridge University Press, 261 pp.

Rees, D., R. G. Roper, K. H. Lloyd and C. H. Low, 1972: Determination of the structure of the atmosphere between 90 and 250 km by means of contaminant releases at Woomera. *Phil. Trans. Roy. Soc. London*, **A271**, 531–666.

Rosenberg, N. W., 1968: Statistical analysis of ionospheric winds —II. *J. Atmos. Terr. Phys.*, **30**, 907–917.

Stommel, H., 1965: *The Gulf Stream.* 2nd ed. University of California Press, Berkeley, 248 pp.

Tanaka, H., 1975: Turbulent layers associated with a critical level in the planetary boundary layer. *J. Meteor. Soc. Japan*, **52**, 425–439.

Thorpe, S. A., 1973: Turbulence in stably stratified fluids: A review of laboratory experiments. *Bound.-Layer Meteor.*, **5**, 95–119.

Woods, J. D., and R. L. Wiley, 1972: Billow turbulence and ocean microstructure. *Deep-Sea Res.*, **19**, 87–121.